

Modified Sternglass theory for the emission of secondary electrons by fast-electron impact

David M. Suszcynsky and Joseph E. Borovsky

Space Plasma Physics Group, Los Alamos National Laboratory, Los Alamos, New Mexico 87545

(Received 4 November 1991)

The Sternglass theory [Sternglass, *Phys. Rev.* **108**, 1 (1957)] for fast-ion-induced secondary-electron emission from metals has been modified to predict the secondary-electron yield from metals impacted by energetic (several keV to about 200 keV) electrons. The primary modification of the theory accounts for the contribution of the backscattered electrons to the production of secondary electrons based on a knowledge of the backscattered-electron energy distribution. The modified theory is in reasonable agreement with recent experimental data from gold targets in the 6–30-keV electron energy range.

PACS number(s): 79.20.Hx, 79.20.Nc, 79.20.Rf, 34.50.Bw

I. INTRODUCTION

A. Secondary-electron emission

When an energetic charged particle impacts a solid, secondary electrons are emitted as a result of energy-transfer processes between the charged particle and the electrons in the solid [Figs. 1(a) and 1(b)]. This emission of secondary electrons is quantified in terms of the secondary-electron (SE) yield of the solid Y , which is the number of secondary electrons emitted per incident charged particle.

Theoretical treatments of secondary-electron emission have been based on many different mechanisms. For example, ion-induced secondary-electron emission has been treated in the 1–100-keV energy range by Parilis and Kishinevskii [2] based on an Auger recombination mechanism and Ghosh and Khare [3] have developed a theory valid at high energies (\geq a few MeV) by relating the yield to the ionization cross section. Electron-induced secondary-electron emission has been described by the elementary theories of Salow [4], Baroody [5], and Bruining [6]. Kanaya and Kawakatsu [7] have modified these results by using a Lindhard power potential to describe

SE emission from metals due to both primary and backscattered electrons, and Kanaya, Ono, and Ishigaki [8] later extended this approach to include insulators. Comprehensive transport theories that are applicable to both electron-induced and ion-induced emission have been presented by Schou [9] and by Rosler and Brauer [10]. The absence of a definitive theory to describe either ion-induced or electron-induced secondary-electron emission is testament to the complex mechanisms involved in the emission process.

B. The Sternglass theory for ion-induced secondary-electron emission

A well-known and particularly useful theory for the emission of secondary electrons from metals induced by energetic ions (\geq a few MeV) was proposed by Sternglass [1] in 1957. In this approach, the emission of secondary electrons [Fig. 1(b)] is described as a three-stage process consisting of (i) the liberation of target electrons by projectile ionization of target atoms, (ii) the migration of these electrons to the target surface, and (iii) the escape of the liberated electrons through the target surface potential barrier. Because the theory is limited to high-velocity ions, the projectile range in the target is much greater than the secondary-electron generating depth d_s . Therefore, to a good approximation, the energy loss of the projectile per unit path length (i.e., the stopping power) can be viewed as a constant within this depth.

In the Sternglass theory, the secondary-electron yield is proportional to the stopping power of the target material and is given by

$$Y_{\text{ion}} = \frac{Pd_s}{E_* \cos\theta} \left[\frac{dE}{dx} \right]_{\text{ion}}, \quad (1)$$

where $P \sim \frac{1}{2}$ is the probability that an ionization electron liberated from a depth d_s will reach the surface and escape, $d_s \sim 5-50 \text{ \AA}$ is the mean escape depth of the secondary electrons and is on the order of the mean free path of a slow electron, θ is the angle between the incident ion's velocity vector and the surface normal of the ma-

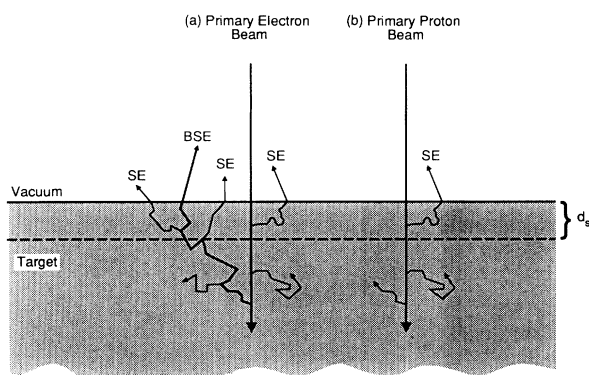


FIG. 1. Diagram showing the generation of secondary electrons (SE's) from both (a) electron impact and (b) proton impact and their subsequent migration to the target surface. The production of secondary electrons from backscattered electrons (BSE's) must be accounted for in the case of electron impact.

terial, and $E_* \sim 25$ eV is the mean energy deposited by the fast ion into the target to produce one ionization pair. $(dE/dx)_{\text{ion}}$ is the electronic-stopping power of the target material and for high-velocity ions is given by [11]

$$\left(\frac{dE}{dx} \right)_{\text{ion}} \simeq - \frac{4\pi(ze)^2 e^2}{m_e v^2} nZ \ln \left[\frac{2m_e v^2}{I} \right], \quad (2)$$

where v and z are the ion velocity and ion charge state, I is the mean excitation potential of the target material, Z and n are the atomic number and number density of the target material, e is the electronic charge, m_e is the mass of the electron, and the “ \simeq ” sign indicates the exclusion of higher-order correction terms in the \ln factor [12]. Basically, $(d_s/\cos\theta)(dE/dx)$ is the amount of energy deposited by the incident ion within d_s of the surface.

The limitations of the Sternglass theory, as with all theories on secondary-electron emission, lie in the simplifying assumptions, namely, the neglect of electron capture and loss effects, the assumption of a constant dE/dx , and the difficulty in assigning accurate values to the parameters P , d_s , and E_* . The effects of the first two points are minimized for the high primary particle energies for which the theory was developed. In addition, the theory neglects the production of secondary electrons by the decay of plasmons and oversimplifies the analysis of distant collisions (small energy transfer between the primary electron and lattice electron) and close collisions (large energy transfer between the primary electron and lattice electron) [13]. The distant collisions directly produce slow secondary electrons and the close collisions produce energetic, forward-scattered electrons (“ δ rays”), which in turn produce secondary electrons in higher-order collisions. Sternglass shows that the production of secondary electrons by δ rays is negligible when the penetration distance of the δ rays L_δ is much greater than the mean free path for collisions for a secondary electron L_s [see Eq. (18a) of Sternglass [1]]. Consequently, in the limit of high primary particle velocities, the contribution by the δ rays to the production of secondary electrons is small and can be neglected. Despite the approximations of the Sternglass theory, its continued use has been warranted by its ability to accurately and simply describe available experimental data [12,14,15].

The purpose of this paper is to modify the Sternglass theory to describe not only ion-induced secondary-electron emission but also electron-induced emission. The modification is motivated by the physical insight provided by the theory into the secondary-electron emission process, the theory’s effectiveness in describing high-velocity emission [12,14,15], its simplicity, and the convenience of having one theory which describes both electron-induced and ion-induced secondary-electron emission. The modification accounts for the production of secondary electrons by the backscattered electrons [16], as well as by the primary electrons. Section II presents the details of the modification and is followed in Sec. III by a comparison of the modified theory to the available experimental results in the MeV/amu-energy range. A summary appears in Sec. IV.

II. MODIFICATION OF THEORY

When a solid is impacted by an ion [Fig. 1(b)], the total yield \mathcal{Y} of electrons from the surface is just equal to the secondary-electron yield of the solid as given by Eq. (1):

$$\mathcal{Y} = Y_{\text{ion}}. \quad (3)$$

In contrast, an important feature of electron-induced emission [Fig. 1(a)] is that some of the incident electrons are backscattered from the solid [16–18]. In this case, secondary electrons are then produced by both incident and backscattered electrons and the total yield of electrons from the target is

$$\mathcal{Y} = Y_{e^-} + Y_r + r, \quad (4)$$

where Y_{e^-} is the secondary-electron yield of the solid due to the incident electrons passing through the surface, Y_r is the secondary-electron yield of the solid due to the backscattered electrons passing back through the surface, and r is the reflection coefficient and represents the number of backscattered electrons per incident electron. The reflection coefficient r can be routinely calculated for the elements from an analytic expression published by Hunger and Kuchler [19].

In order to describe electron-induced secondary-electron emission, the modified version of the Sternglass theory must be able to evaluate the terms Y_{e^-} and Y_r in Eq. (4). In the framework of the Sternglass theory, an incident electron will produce secondary electrons in the same manner as does an incident ion since the yield is a function of only the charge and velocity of the incident particle. Y_{e^-} can then be expressed as

$$Y_{e^-} = \frac{Pd_s}{E_* \cos\theta} \left(\frac{dE}{dx} \right)_{e^-}, \quad (5)$$

where now [11,20]

$$\left(\frac{dE}{dx} \right)_{e^-} \simeq - \frac{4\pi(ze)^2 e^2}{m_e v^2} nZ \left[\ln \left(\frac{2m_e v^2}{I} \right) - 1.2329 \right]. \quad (6)$$

Here $z = -1$ (incident electron) and the 1.2329 term accounts for the indistinguishability of the incident and target electrons following a collision and for the reduced mass of this two-electron system. The evaluation of Y_r , on the other hand, must take into account the energy and angular distributions of the backscattered electrons. We evaluate this term by essentially reapplying the method used by Sternglass in evaluating Y_{ion} in Eq. (1) with the exception that we now integrate over the distribution of backscattered electrons in both energy and angle.

When a normally incident beam of electrons impacts a solid, backscattered electrons are produced with a distribution $f(E_{\text{BSE}}, \theta)$ in both energy and angle. This distribution is given by

$$f(E_{\text{BSE}}, \theta) = C_n W(E_{\text{BSE}}) \cos\theta, \quad (7)$$

where θ is the angle between the backscattered-electron

trajectory and the normal to the solid, E_{BSE} is the backscattered-electron energy, $W(E_{\text{BSE}})$ is a function describing the energy distribution of backscattered electrons, and C_n is a normalization constant that is determined by integrating $f(E_{\text{BSE}}, \theta)$ over all angles and energies and setting the result equal to the reflection coefficient r :

$$\begin{aligned} r &= \int d\Omega \int dE_{\text{BSE}} f(E_{\text{BSE}}, \theta) \\ &= C_n \int_{E_{\text{max}}}^{E_0} dE_{\text{BSE}} \int_0^{2\pi} d\phi \int_0^{\pi/2} d\theta W(E_{\text{BSE}}) \cos\theta \sin\theta. \end{aligned} \quad (8)$$

In the limits of the integral, E_0 is the incident electron energy and E_{max} is the energy at which the maximum of the dE/dx curves occurs. Since the Sternglass theory is only valid for energies above the maximum of dE/dx (i.e., only valid when the range of the incident electron is greater than d_s), the modified theory will only be accurate if about 95% or more of the backscattered electrons have energies above E_{max} . This condition is easily met since the majority of backscattered electrons usually have energies that are a large fraction of the incident-electron energy [18]. Since the depth at which an electron is backscattered is so much greater than d_s , we can make the approximation that a backscattered electron passes straight through the emission region of depth d_s and that each backscattered electron has a constant energy during its trajectory through this region. If we once again apply the Sternglass theory, this time to the backscattered electrons rather than the primary electrons, the term Y_r can then be written as

$$\begin{aligned} Y_r &= \frac{Pd_s}{E_*} \int_{E_{\text{max}}}^{E_0} dE_{\text{BSE}} \left[\frac{dE_{\text{BSE}}}{dx} \right]_e \\ &\quad \times \int_{-\pi/2}^{\pi/2} d\theta f(E_{\text{BSE}}, \theta) \frac{1}{\cos\theta}, \end{aligned} \quad (9)$$

where the $1/\cos\theta$ factor accounts for the increased path length of the backscattered electrons through the secondary-electron generating depth d_s [21] and $f(E_{\text{BSE}}, \theta)$ is given by Eq. (7). Equations (4), (5), and (9) collectively represent the modified Sternglass theory for electron-induced secondary-electron emission.

In the original Sternglass theory [1], two types of collisional processes were attributed to the production of secondary electrons: collisions between the primary and lattice electrons that (i) directly resulted in secondary electrons and (ii) generated δ rays that in turn produced secondary electrons through higher-order collisions. For energetic primary electrons, the resulting δ rays have a negligible contribution to the production of secondary electrons, partly because of their forward scattering in a direction *opposite* to the direction of secondary-electron emission (i.e., the same direction as the primary electron beam). However, when modifying the Sternglass theory to account for the production of secondary electrons by backscattered electrons, the forward scattering of the δ rays by the backscattered electrons is now in the *same* direction of travel as the secondary electron emission and

the effect of the δ rays in producing secondary electrons becomes somewhat more pronounced. This effect can be quantified somewhat by considering the experimental results of Reimer and Drescher [22]. Their experiments studied the secondary-electron production from primary electrons exiting thin gold and aluminum targets. Their results (Fig. 5 of Reimer and Drescher [22]) show that the secondary-electron yield for 9.3-keV electrons exiting a thin film of aluminum increases from 0.21 to a maximum of 0.31 as the film thicknesses is increased from ~ 0 to 3700 Å. This increase in yield is due to the decrease in energy of the transmitted electrons and to the production of secondary electrons by the δ rays. However, since the range of a 9.3-keV electron is roughly 10 000 Å and since $Y \sim dE/dx$, it is clear that the majority of the increase in the yield as the sample thickness is increased is due to the slowing down of the transmitted electrons and that the δ rays must contribute a very small amount to this increase. In light of these results, we make the approximation that the contribution of the δ rays to the production of secondary electrons is negligible within the uncertainties of the modified theory and therefore no attempt is made in the modified theory to account for them.

III. COMPARISON WITH EXPERIMENTAL DATA

The comparison of the modified theory to experimental data is illustrated in Fig. 2. Previously published secondary-electron yield measurements are shown for both protons [14,15,23] and electrons [15,23] normally incident on gold targets over the same range of particle velocities. Both data sets were collected using the same experimental technique. The secondary-electron yield ($Y_e + Y_r$) is plotted as a function of incident particle energy. For convenience, the x axis is scaled in both MeV/amu and keV/emu units where emu represents "electron mass units." The electron-induced yields are consistently larger than the proton-induced yields for a given energy because of the contribution of the backscattered electrons to the production of secondary electrons.

Details of the target-cleaning technique and an assessment of the reproducibility of the data can be found in Suszczyński and Borovsky [15]. Based on the scatter of the data points, the reproducibility of the data, and the comparison of the data to previous authors' measurements, the uncertainty in any one measurement is estimated to be about 20%.

Since P , d_s , and E_* values in the Sternglass theory are invariant to projectile type and velocity and since they are not well defined experimentally, the comparison of the theory to the data is best illustrated with a method that is independent of these values. For the proton data, a one-parameter least-squares fit (dotted line) of the Sternglass theory [Eq. (1)] to the data indicates that $Pd_s/E_* = 1.72 \times 10^{-9}$ cm/eV. This value for Pd_s/E_* is then used in Eqs. (5) and (9) to calculate the predicted yield from electron-induced emission based on the modified Sternglass theory (solid line).

For the function $W(E)$ in Eq. (7), a fifth-order polynomial fit is made to the backscattered-electron energy-distribution plot for platinum found in Sternglass [18]

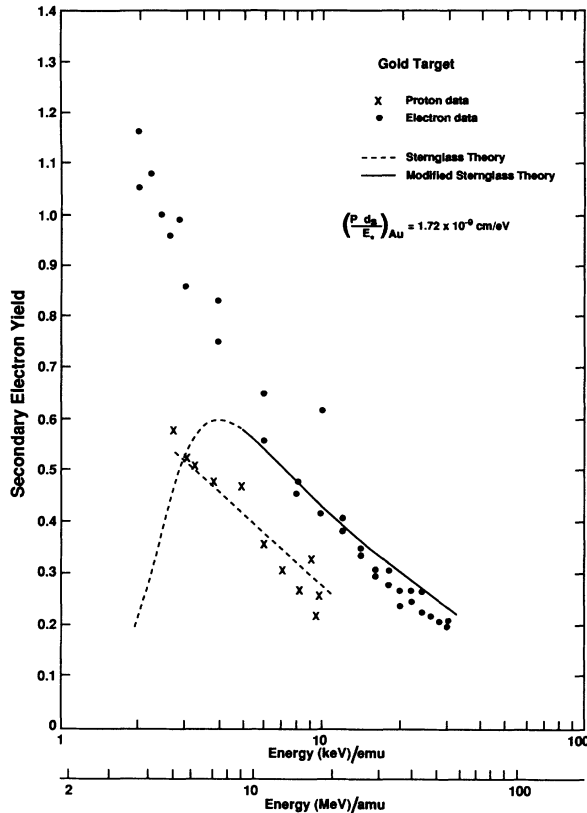


FIG. 2. Secondary-electron yields for gold due to electron impact (●) and proton impact (×) as a function of incident particle velocities. A one-parameter fit of the Sternglass theory to the proton data (dotted line) produces a value of $(Pd_s/E_*)_{Au} = 1.72 \times 10^{-9}$ cm/eV, which is then used to predict the secondary-electron yield for electron impact (solid line) based on the modified Sternglass theory. For gold, $E_{max} = 800$ eV (Ref. [24]) and $I = 770$ eV (Ref. [1]).

(Fig. 3 of this paper). Since the reflection coefficient r and energy distribution $W(E)$ for a given material are primarily a function of Z , the gold ($Z = 79$) distribution is well approximated by the platinum ($Z = 78$) data.

As can be seen in Fig. 2, the prediction of the electron-induced yield based on the modified theory agrees with the gold data to within 10% for electron energies greater than about 8 keV. For energies less than 8 keV, the lower limit of the energy integral, E_{max} , in Eq. (9) begins to exclude a significant portion ($> 5\%$) of the backscattered-electron distribution and results in a breakdown of the theory at lower energies. This part of the curve is dashed to indicate the inability of the theory to account for a significant portion of the backscattered electrons in this energy range. The value of E_{BSE}/E_0 at which this breakdown begins to occur is also indicated by an arrow in Fig. 3.

In general, the lower limit of the energy range over which the modified theory is valid is determined by the Z of the target material. As Z decreases, the mean energy of the backscattered electrons decreases slightly (see Fig. 3), resulting in a populating of the lower energy portion

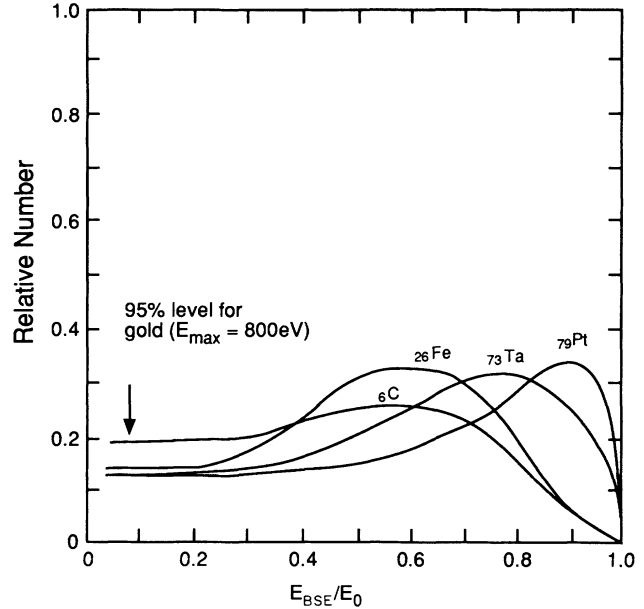


FIG. 3. Energy-distribution curves of backscattered electrons from target materials of various Z values. Data taken over 0.5–2.0-keV energy range from Sternglass (Ref. [18]). Arrow indicates the lower limit of the energy integral [Eqs. (8) and (9)] for the example discussed in the text.

of the backscattered-electron energy distribution. However, since E_{max} also generally decreases with a decrease in Z [24], the slight shifting of the backscatter energy distribution towards a lower energy does not result in an increase in the minimum energy for which the theory is valid. Practically speaking then, a valid lower limit for E_0 is about several keV. The theory is also invalid at very high electron energies ($E_0 \geq 200$ keV) because of relativistic corrections to dE/dx . These corrections become large at $E_0 \approx 500$ keV.

IV. SUMMARY

In summary, the Sternglass theory for secondary-electron emission from metals due to fast-ion impact has been modified to include the case of electron-induced emission. The modified theory is valid for electron energies from several keV (depending on the Z of the metal) to about 200 keV (limited by the onset of relativistic effects). To utilize the modified theory, a knowledge of the backscattered-electron energy distribution is needed in order to quantify the contribution of the backscattered electrons to the production of secondary electrons. Experimental data for backscattered-electron energy distributions can be found in a number of papers [18,21,25–30]. The modified theory agrees with recent secondary-electron yield data for gold to within 10%.

ACKNOWLEDGMENT

This work was supported by the U.S. Department of Energy.

- [1] E. J. Sternglass, *Phys. Rev.* **108**, 1 (1957).
- [2] E. S. Parilis and L. M. Kishinevskii, *Sov. Phys. Solid State* **3**, 885 (1960).
- [3] S. N. Ghosh and S. P. Khare, *Phys. Rev.* **125**, 1254 (1962).
- [4] H. Salow, *Z. Phys.* **41**, 434 (1940).
- [5] E. M. Baroody, *Phys. Rev.* **78**, 780 (1950).
- [6] H. Bruining, in *Physics and Applications of Secondary Electron Emission* (Pergamon, London, 1954), Chap. 6.
- [7] K. Kanaya and H. Kawakatsu, *J. Phys. D* **5**, 1727 (1972).
- [8] K. Kanaya, S. Ono, and F. Ishigaki, *J. Phys. D* **11**, 2425 (1978).
- [9] J. Schou, *Phys. Rev. B* **22**, 2141 (1980).
- [10] M. Rosler and W. Brauer, *Phys. Status Solidi B* **148**, 213 (1988).
- [11] H. A. Bethe and J. Ashkin, in *Experimental Nuclear Physics, Vol. 1*, edited by E. Segre (Wiley, New York, 1953), p. 166.
- [12] J. E. Borovsky and D. M. Suszcynsky, *Phys. Rev. A* **43**, 1416 (1991).
- [13] R. A. Baragiola, E. V. Alonso, J. Ferron, and A. Oliva-Florio, *Surf. Sci.* **90**, 240 (1979).
- [14] J. E. Borovsky, D. J. McComas, and B. L. Barraclough, *Nucl. Instrum. Methods B* **30**, 191 (1988).
- [15] D. M. Suszcynsky and K. E. Borovsky, *Nucl. Instrum. Methods B* **53**, 255 (1991).
- [16] H. Kanter, *Phys. Rev.* **121**, 681 (1961).
- [17] H. Niedrig, *J. Appl. Phys.* **53**, R15 (1982).
- [18] E. J. Sternglass, *Phys. Rev.* **95**, 345 (1954).
- [19] H. J. Hunger and L. Kuchler, *Phys. Status Solidi A* **56**, K45 (1979).
- [20] P. Marmier and E. Sheldon, *Physics of Nuclei and Particles, Vol. 1* (Academic, New York, 1969), p. 171.
- [21] H. Kanter, *Ann. Phys. (Leipzig)* **20**, 144 (1957).
- [22] L. Reimer and H. Drescher, *J. Phys. D* **10**, 805 (1977).
- [23] D. M. Suszcynsky, J. E. Borovsky, and B. L. Barraclough, Los Alamos National Laboratory Report No. LA-11915-MS, 1990 (unpublished).
- [24] N. R. Whetten, in *Handbook of Physics and Chemistry*, 60th ed., edited by R. C. Weast (CRC, Boca Raton, 1979), p. E-379.
- [25] H. Kulenkampff and W. Spyra, *Z. Phys. (Leipzig)* **137**, 416 (1957).
- [26] H. Kulenkampff and K. Ruttiger, *Z. Phys. (Leipzig)* **137**, 426 (1957).
- [27] E. H. Darlington, *J. Phys. D* **8**, 85 (1975).
- [28] W. Bothe, *Z. Naturforsch. A* **4**, 542 (1949).
- [29] H. E. Bishop, in *X-Ray Optics and Microanalysis*, edited by R. Castaing, P. Deschamps, and J. Philibert (Hermann, Paris, 1966), p. 153.
- [30] T. Matsukawa, R. Shimizu, and H. Hashimoto, *J. Phys. D* **7**, 695 (1974).

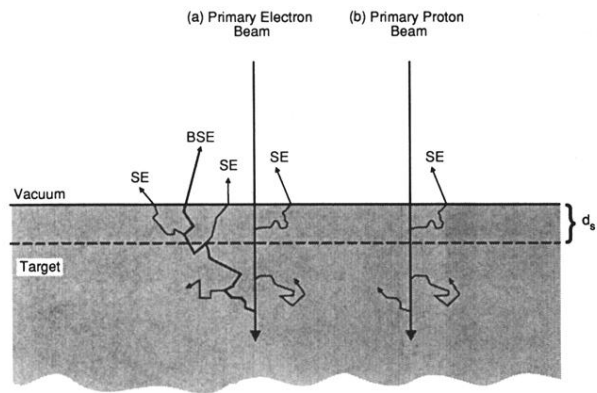


FIG. 1. Diagram showing the generation of secondary electrons (SE's) from both (a) electron impact and (b) proton impact and their subsequent migration to the target surface. The production of secondary electrons from backscattered electrons (BSE's) must be accounted for in the case of electron impact.